

Mechanical properties and microstructure of reaction sintered β' -sialon ceramics prepared by a slip casting method

SEIJI HAYAMA, TAKAKUNI NASU, MASAKUNI OZAWA, SUGURU SUZUKI
Ceramic Research Laboratory, Nagoya Institute of Technology, 10-6-29 Asahi-ga-oka, Tajimi, Gifu 507, Japan

Reaction sintered β' -sialon ceramics $\text{Si}_{6-z}\text{Al}_z\text{O}_z\text{N}_{8-z}$, were prepared by slip casting from α - Si_3N_4 , Al_2O_3 , and AlN starting powders. The mechanical properties and microstructures of sintered bodies were investigated as a function of composition (varying the z value). The maximum value of the flexural strength, ~ 600 MPa, and fracture toughness, ~ 4.1 MPa $\text{m}^{1/2}$ were observed in the z range of 0.5–1. In the z value range of 2–4, the mechanical properties decreased drastically. This phenomenon is attributed to the variation of fracture energy, which is greatly affected by the sintered crystallite size.

1. Introduction

The β' -sialon ceramics with the chemical formula $\text{Si}_{6-z}\text{Al}_z\text{O}_z\text{N}_{8-z}$ where $0 < z \leq 4.2$ find application as high temperature structural materials due to its high oxidation resistance as well as its excellent resistance to erosion with molten metals at high temperatures [1–3]. The β' -sialons are produced from Si_3N_4 , Al_2O_3 and AlN starting materials that are densified by pressure sintering (a hot press or a hot isostatic press) [4] or pressureless (reaction) sintering [5–7]. Although pressure sintering creates favourable properties for sintered bodies, the sintering cost is very high, and in addition complicated shapes are difficult to form.

Reaction sintering of a pre-formed body is suited to industrial production because of the ease of fabrication and its low cost. The forming process normally makes use of mechanical presses or a cold isostatic press, however to obtain a high density body, a high pressure apparatus is necessary which involves a high machine cost. However, there is a limit to the shapes that can be produced using this apparatus.

On the other hand, a slip casting method enables us to prepare relatively high density bodies and complicated shapes at a low cost. In the present paper, the mechanical properties and microstructures of reaction sintered β' -sialons, $\text{Si}_{6-z}\text{Al}_z\text{O}_z\text{N}_{8-z}$, prepared by slip casting at various compositions i.e. z values have been investigated.

2. Experimental procedure

2.1. Materials

The starting powders used to prepare the sialon ceramics were α - Si_3N_4 (SN-9S, Denki Kagaku Kogyo Co. Ltd., Japan with a mean particle size (mps); 0.8 μm), Al_2O_3 (AL-160SG, Showa Denko Co. Ltd., Japan with a mps; 0.5 μm), and AlN (UF, Toyo

Aluminium Co. Ltd., Japan with a mps; 1.5 μm). Aqueous slurries for slip casting were prepared from the α - Si_3N_4 , Al_2O_3 and AlN at the compositions listed in Table I. In addition 3 wt% Y_2O_3 (Y-F, Mitsubisikasei Ltd., Japan, with a mps; 1 μm) was used as a sintering aid and 0.4 wt% of polycarboxylic ammonium salt (RFA, Sunnopco Ltd., Japan) was added as a dispersant. The solid concentration was determined to be 40 vol% in all slurries. Each component was homogeneously mixed using a ball mill (polyethylene pot and resin coating ball, 17 mm dia.) for 2 h at a fixed temperature. The slurries, after de-airing, were poured into the plaster moulds and $90 \times 20 \times 7$ mm green bodies were removed from the moulds after standing for 24 h. The green bodies were dried at 110 $^\circ\text{C}$ for 24 h, and then sintered at 1750 $^\circ\text{C}$ for 6 h in a nitrogen atmosphere (0.15 MPa).

2.2. Analysis of the sintered bodies

The lattice parameters of the sintered bodies were determined by X-ray diffraction (Rigaku, RINT-1100K) from the (301), (002), (321), (411) and (212) Miller indices. The apparent densities were determined in water using the Archimedes technique and these values were compared with the theoretical values calculated from the lattice parameters. The flexural strength was measured by a three-point flexural method on specimens with a 3.0 mm thickness and a 4.0 mm width, with a span of 30 mm and a cross head speed of 0.5 mm min^{-1} . The measurements were performed in air at room temperature. The fracture toughness was determined using the Chevron-notched-beam method [8] on specimens of dimension 3.0×4.0 mm with a notch at the centre of the specimen, a span of 20 mm and a cross head speed of 0.005 mm min^{-1} . The room temperature Young's

TABLE I The mixing ratios of the starting powders at the β' -sialon compositions, $\text{Si}_{6-z}\text{Al}_z\text{O}_z\text{N}_{8-z}$

z -value	Si_3N_4 (wt %)	Al_2O_3 (wt %)	AlN (wt %)
0	100.0	0.0	0.0
0.5	91.5	6.1	2.4
0.7	88.1	8.5	3.4
0.9	84.7	10.9	4.4
1.0	83.0	12.1	4.9
1.1	81.3	13.3	5.3
1.3	78.0	15.7	6.3
1.5	74.6	18.1	7.3
2.0	66.2	24.1	9.7
3.0	49.5	36.0	14.5
4.0	32.9	47.9	19.2

modulus was measured using the ultrasonic pulse echo method. The microstructure of the fracture face was observed by scanning electron microscopy (SEM: Jeol, SM-6100).

3. Results and discussion

The X-ray diffraction patterns of the sintered bodies for z values of 0, 0.5, 1, 2, 3 and 4 are shown in Fig. 1. Only peaks that can be assigned to β' -sialon are observed for z values between 0.5–3. However, for z values of 0 and 4, minor peaks belonging to $\text{Y}_3\text{Si}_3\text{N}_4\text{O}_3$ and $\alpha\text{-Al}_2\text{O}_3$ are observed, respectively. Fig. 2 shows the lattice parameters for the various z values, the relationship between the measured values is shown by the solid straight line. For the a - and c -axes, the measured lattice parameters are related to the z values by the following linear equations:

$$a(\text{nm}) = 0.7600 + 0.003079z (\pm 0.0004) \quad (1)$$

$$c(\text{nm}) = 0.2904 + 0.002673z (\pm 0.0003) \quad (2)$$

where the error is the standard deviation obtained from the least-square fitting of the experimental data. Land, *et al.* [9], and Ekström, *et al.* [10], have also reported linear variations, that are shown as the dashed lines in Fig. 2, that closely agree with the present results.

Fig. 3 shows the relationship between the theoretical density calculated from the lattice parameters and the apparent density measured by the Archimedes method. The apparent densities for z values near 1 are closest to the theoretical densities, for $z = 1$ the relative density is 99.3% which is the highest value of the obtained relative densities. As z increased to 3, the relative density decreases to 97.9%, but as z increases further to 4, the value becomes slightly closer to the theoretical value. This is thought to be due to the presence of $\alpha\text{-Al}_2\text{O}_3$ as was shown in Fig. 1. On the other hand, for $z = 0$, the relative density is only 91.9%, this is believed to be a result of only using Y_2O_3 as a sintering aid thus an insufficient transient liquid phase is formed during sintering, and thus full sintering is not attained.

The Young's modulus (E) values are shown in Fig. 4. The values almost fit a straight line with a very

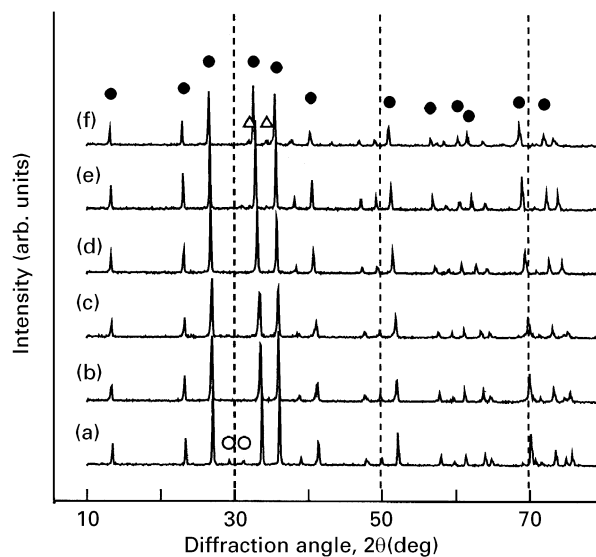


Figure 1 X-ray diffraction patterns of reaction sintered β' -sialon ceramics prepared by slip casting. (a) $z = 0$, (b) $z = 0.5$, (c) $z = 1.0$, (d) $z = 2.0$, (e) $z = 3.0$ and (f) $z = 4.0$. Key: (●) β' -sialon, (△) Al_2O_3 and (○) $\text{Y}_2\text{Si}_3\text{N}_4\text{O}_3$.

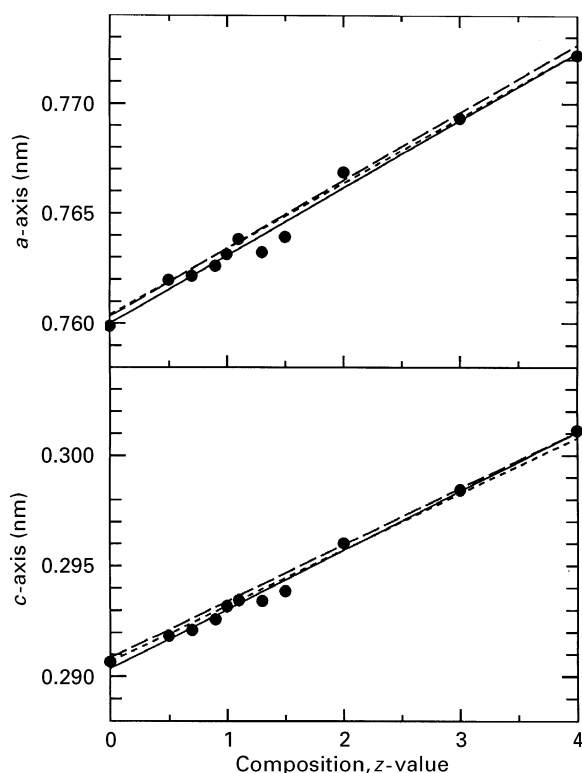


Figure 2 The lattice parameters of a hexagonal β' -sialon phase as functions of the z -value. Key: (---) Ekström *et al.* [10] and (-.-.-) Land *et al.* [9].

minor decrease in the Young's modulus as z is increased with the exception of the value at $z = 0$. The results closely agree with the published data of Wills *et al.* [5] of 234 GPa at $z = 2$ and the data of Tani *et al.* [11] measured on hot pressed samples of 285 GPa for $z = 1$, 229 GPa for $z = 3$. It is believed that the variation in the Young's modulus is closely related to the density which was shown in Fig. 3.

The flexural strength, fracture toughness and fracture energy are shown in Table II. The highest flexural

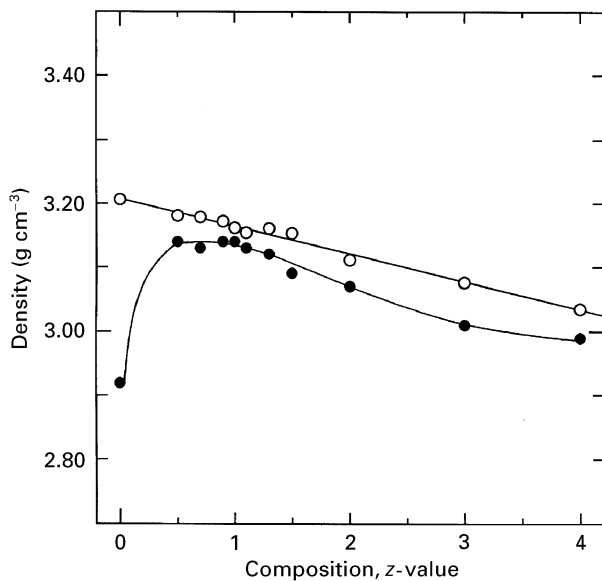


Figure 3 The (○) calculated and (●) measured density as a function of the z -value of reaction sintered β' -sialon prepared by slip casting.

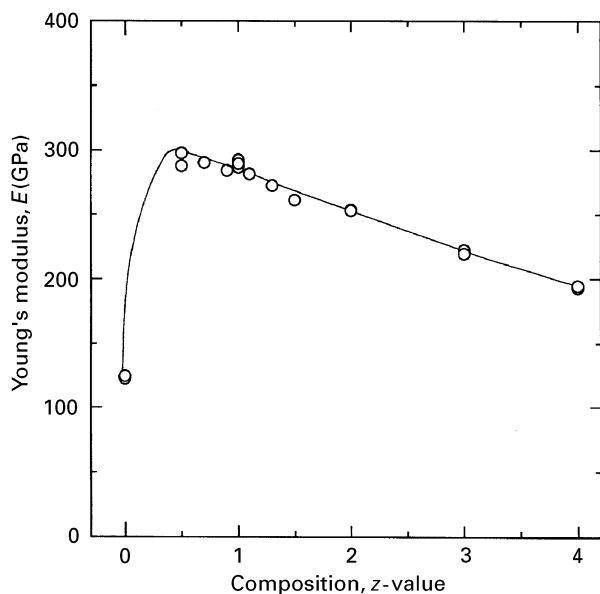


Figure 4 Relation between the z -value and the Young's modulus of reaction sintered β' -sialon prepared by slip casting.

strength values of approximately 600 MPa are obtained for z values between 0.5–1. These values are comparable with those measured on a hot pressed sample [11]. When the z value exceeds 1, the flexural strength drastically decreases, with values of 233 MPa for $z = 3$ and 165 MPa for $z = 4$.

With reference to the flexural strength values of reaction sintered β' -sialon reported by Mitomo *et al.* [12], of 320 MPa for $z = 1.5$ and 390 MPa for $z = 2.0$ and Wills *et al.* [5, 6], of 377 MPa for $z = 1$ and 352 MPa for $z = 2$, the present values are higher than these values for z values between 0.5–1.5. On the other hand, for z values between 2–4, the values are lower. Thus it appears that the composition has a greater affect on the flexural strength than has been previously thought.

The fracture toughness (K_{IC}) varies in the same manner as the flexural strength as a function of the z

TABLE II The mechanical properties of reaction sintered β' -sialon, $\text{Si}_{6-z}\text{Al}_z\text{O}_2\text{N}_{8-z}$, prepared by slip casting

z -value	Flexural strength (MPa)	Fracture toughness ($\text{MPa m}^{1/2}$)	Fracture energy (J m^{-2})
0	307.4 ± 47.0	2.92 ± 0.16	34.4 ± 3.8
0.5	604.3 ± 56.4	4.13 ± 0.49	29.1 ± 7.3
0.7	564.3 ± 99.2	3.53 ± 0.30	21.5 ± 3.8
0.9	607.4 ± 47.1	3.74 ± 0.32	24.6 ± 4.4
1.0	524.0 ± 74.2	3.18 ± 0.20	17.5 ± 2.3
1.1	497.9 ± 87.9	3.51 ± 0.40	21.9 ± 5.2
1.3	483.8 ± 64.7	3.03 ± 0.23	16.9 ± 2.7
1.5	419.4 ± 46.2	2.63 ± 0.17	13.2 ± 1.8
2.0	355.9 ± 42.7	1.80 ± 0.24	6.4 ± 1.8
3.0	232.6 ± 27.4	1.35 ± 0.11	4.1 ± 0.7
4.0	164.5 ± 21.2	1.51 ± 0.29	5.9 ± 2.4

value. The highest fracture toughness value of $4.1 \text{ MPa m}^{1/2}$ is obtained at $z = 0.5$ and a steep decrease in the values is observed beyond this point. The lowest value of $1.4 \text{ MPa m}^{1/2}$ is observed at $z = 3$.

The fracture energy (γ_s) is obtained from the equation [13]:

$$K_{IC} = (2E\gamma_s)^{1/2} \quad (3)$$

The fracture energy has its maximum value at $z = 0$ at a value of 34.4 J m^{-2} and then decreases linearly as a function of z to $z = 3$. The values are 20 J m^{-2} for $z = 1$, 6.4 J m^{-2} for $z = 2$ and the lowest value is observed at $z = 3$. These values show a similar trend to the published values of 14.5 J m^{-2} for $z = 1$ and 9.8 J m^{-2} for $z = 2$ of Wills *et al.* [6]. It is believed that the fracture energy is influenced by the composition (z value) in a similar manner as the mechanical strength and fracture toughness properties of the sintered bodies.

To complete the changes in the mechanical properties with the sample microstructure, SEM photographs of the fracture face of the samples were taken and are shown in Fig. 5(a–f). At $z = 0$, the microstructure is rather porous but fully grown very fine and elongated crystals can be observed which make the complex configuration between the crystals rather strong.

For $z = 0.5$ –1, the microstructure becomes dense with average crystallite sizes (diameters) of 1–1.5 μm , at the same time many pull-out marks of elongated crystals are observed in the structure. Fracture patterns associated with transgranular and intergranular fracture are both observed. For $z = 2$, the crystallite sizes become larger with average crystal sizes of 3–4 μm , however, elongated crystals become difficult to observe. At $z = 3$, the crystallite sizes reach average sizes greater than 6 μm , making the boundaries of the crystals difficult to observe. This behaviour seems to be suggestive of transgranular fracture. When $z = 4$, the fracture face looks like glass, and thus the crystallite sizes could not be estimated.

Comparing these results with those reported by Tani *et al.* [11], of crystallite sizes of 1 μm for $z = 1$ and 5 μm for $z = 4$, the present crystals are larger in the high z value range. Based on these results, it

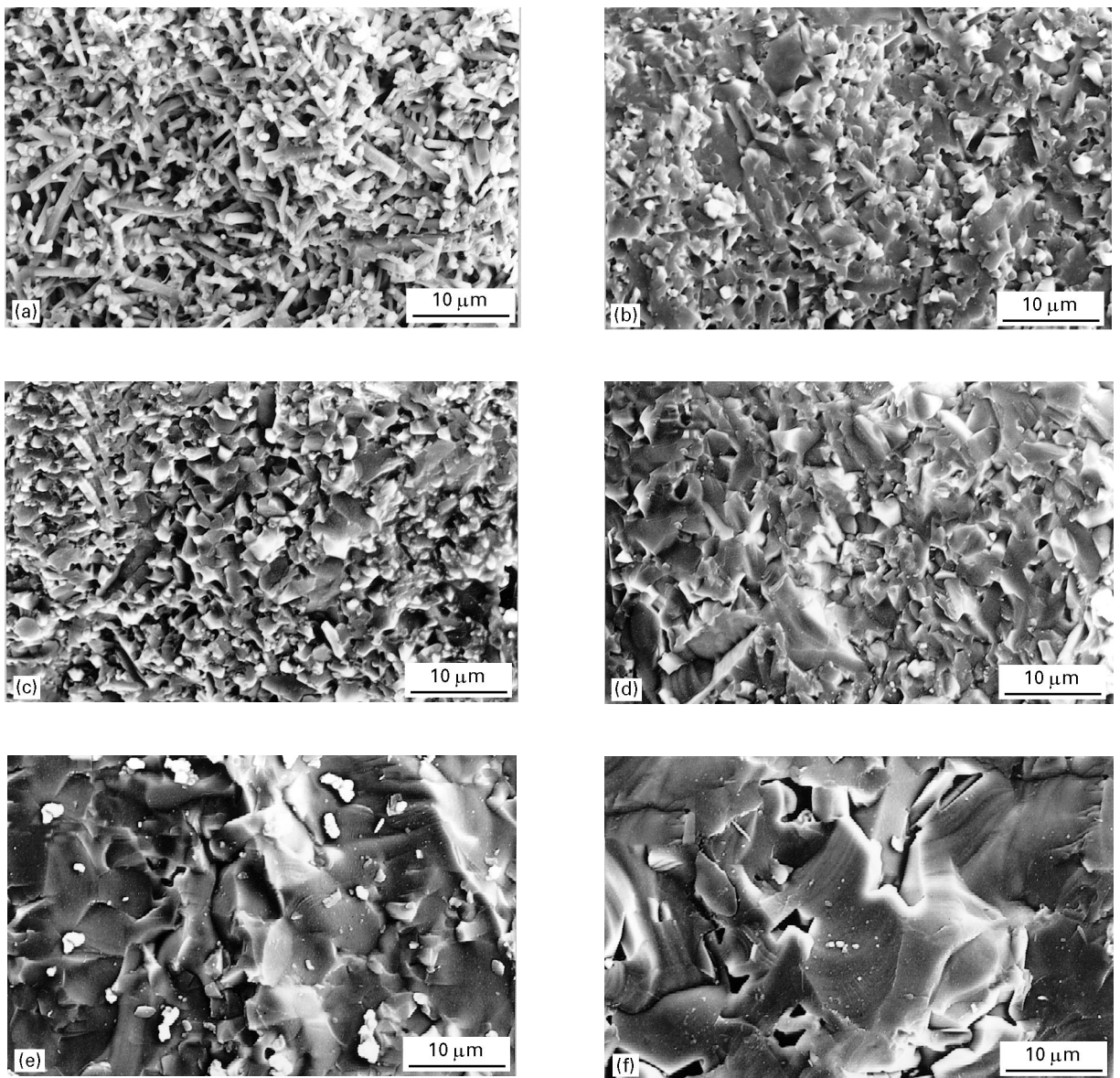


Figure 5 Scanning electron micrographs of the fracture surface of β' -sialon with the z -value: (a) $z = 0$, (b) $z = 0.5$, (c) $z = 1$, (d) $z = 2$, (e) $z = 3$ and (f) $z = 4$.

appears that the crystallite sizes are closely related to the fracture energy of the sintered bodies, i.e., the change in crystallite size produces a change in the fracture energy thereby affecting the mechanical properties. The relationship between the crystallite size and fracture energy is shown in Fig. 6. The measurements of crystallite size (diameter) are performed by a linear increment method. From Fig. 6, the relationship between fracture energy and crystallite size (D) can be expressed in the following form:

$$\gamma_s = kD^{-A} \quad (4)$$

where k and A are experimental constants having the values $k = 25.8$ and $A = 0.97$. This relationship implies a large decrease in the fracture energy with an increase in the crystallite size. As a rule, the fracture energy of ceramics is greatly affected by the configuration of its microstructure, a polycrystalline body compared to a single crystal body will in practice give a much higher fracture energy. This is attributed to the fact that the polycrystalline body shows irreversible

energy scattering on the crack due to a complicated fracture process such as crack branching and plastic deformation on the crack tip. Coppola and Bradt [14] have reported a comparison of fracture energies of several types of silicon carbide specimens. They measured values of $14\text{--}37 \text{ J m}^{-2}$ for a notched-beam test and $11\text{--}83 \text{ J m}^{-2}$ for a work-of-fracture test. The increase in fracture energy was shown to be associated with a change from transgranular to intergranular fracture, with small sized crystallite shown in intergranular fracture. They also found that the presence of elongated crystallites and a bimodal-grain-structure produced a higher fracture energy. Thus the small crystallite size in the low z value range shows a complicated fracture behaviour associated with a polycrystalline body, while the large crystallite size in the high z value range shows smooth fracture similar to a single crystal due to the disappearance of elongated crystals and an increase of transgranular fracture.

The present results show that reaction sintered β' -sialon prepared by slip-casting has mechanical

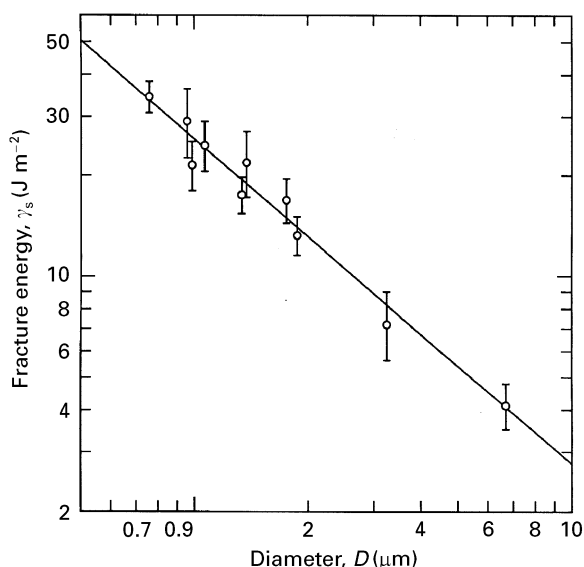


Figure 6 Fracture energy of β' -sialon ceramics as a function of the crystallite size.

properties comparable to previously published results in the low z value range, but in the high z value range, they indicate poor properties. To improve the mechanical properties in the high z value range, then the fracture energy could be increased by inhibiting crystal growth and/or by forming a high-energy grain boundary from the secondary phases.

4. Conclusions

The mechanical properties and microstructure of reaction sintered β' -sialon, $\text{Si}_{6-z}\text{Al}_z\text{O}_z\text{N}_{8-z}$, prepared by a slip casting technique were investigated as a function of the z value. The results are as follows:

(1) The maximum value of the flexural strength, 600 MPa, is obtained in the z range of 0.5–1.

(2) The fracture toughness has a maximum value at $z = 0.5$ of $4.1 \text{ MPa m}^{1/2}$.

(3) The Young's modulus changes from 300 to 200 GPa with an increase of z from 0.5–4.

(4) The fracture energy, γ_s , decreases from 34 to 4 J m^{-2} as z increases.

(5) The fracture energy, γ_s , decreases with increasing crystallite size, D . This relationship can be expressed as $\gamma_s = 25.8 D^{-0.97}$.

(6) The lattice parameters are related to the z value by the following linear equations: $a(\text{nm}) = 0.7600 + 0.003079z$, $c(\text{nm}) = 0.2904 + 0.002673z$.

References

1. K. H. JACK, *J. Mater. Sci.* **11** (1976) 1135.
2. L. J. GAUCKLER, H. L. LUKAS and G. PETZOW, *J. Amer. Ceram. Soc.* **58** (1975) 346.
3. M. B. TRIGG and D. B. ELLSON, *Brit. Ceram. Trans. J.* **87** (1988) 153.
4. M. MITOMO, N. KURAMOTO, M. TSUTSUMI and H. SUZUKI, *Yogyo-Kyokai-shi* **86** (1978) 526.
5. R. R. WILLS, R. W. STEWART and J. M. WIMMER, *J. Amer. Ceram. Soc.* **60** (1977) 64.
6. *idem*, *Ceramic Bull.* **56** (1977) 194.
7. M. MITOMO, N. KURAMOTO and Y. INOMATA, *J. Mater. Sci.* **14** (1979) 2309.
8. D. MUNZ, G. HIMSOLT and J. ESCHWEILER, *J. Amer. Ceram. Soc.* **63** (1980) 341.
9. P. L. LAND, J. M. WIMMER, R. W. BURNS and N. S. CHOUDHURY, *ibid.* **61** (1978) 56.
10. T. EKSTRÖM, P. O. KALL, M. NYGREN and P. O. OLSSON, *J. Mater. Sci.* **24** (1989) 1853.
11. E. TANI, S. UMEBAYASHI, K. OKUZONO, K. KISHI and K. KOBAYASHI, *Yogyo-Kyokai-shi* **93** (1985) 370.
12. M. MITOMO, N. KURAMOTO and Y. INOMATA, *ibid.* **88** (1980) 489.
13. G. R. IRWIN, *J. Appl. Mech.* **29** (1962) 651.
14. J. A. COPPOLA and R. C. BRADT, *J. Amer. Ceram. Soc.* **55** (1972) 455.

Received 24 October 1995

and accepted 10 February 1997